

Thermoelectric properties of the n-type 85% Bi₂Te₃-15% Bi₂Se₃ alloys doped with SbI₃ and CuBr

D. B. HYUN, J. S. HWANG, B. C. YOU

Division of Metals, Korea Institute of Science and Technology, Seoul 136-791, Korea
E-mail: dbhyun@kistmail.kist.re.kr

T. S. OH

Dept. of Metallurgy and Materials Science, Hong Ik University, Seoul 121-791, Korea

C. W. HWANG

Thermotek, LTD, Sungnam 463-070, Korea

The temperature dependence of the Hall mobility, Seebeck coefficient, electrical resistivity, thermal conductivity, and figure-of-merit of the SbI₃ and CuBr-doped 85% Bi₂Te₃-15% Bi₂Se₃ single crystals have been characterized at temperatures ranging from 77 K to 600 K. The scattering parameter in 85% Bi₂Te₃-15% Bi₂Se₃ single crystal was determined as 0.1 from the temperature dependence of the carrier mobility. With increasing the amount of SbI₃ or CuBr doping, the Seebeck coefficient of 85% Bi₂Te₃-15% Bi₂Se₃ decreased and the temperature at which the Seebeck coefficient shows a maximum shifted to higher temperature. Compared to the SbI₃-doped specimens, the CuBr-doped single crystals exhibited higher $(m^*/m_0)^{3/2}\mu_c$, implying that CuBr is a more effective dopant to improve the material factor and thus the figure-of-merit of 85% Bi₂Te₃-15% Bi₂Se₃. The maximum figure-of-merit of $2.0 \times 10^{-3}/\text{K}$ and $2.2 \times 10^{-3}/\text{K}$ was obtained for 0.1 wt % SbI₃-doped specimen and 0.03 wt % CuBr-doped specimen, respectively. © 1998 Kluwer Academic Publishers

1. Introduction

Thermoelectric modules utilizing the Peltier effect have been widely applied to cool electronic devices such as integrated circuit packages, laser diodes and infrared detectors, because quick and precise control of temperature is possible with almost no noise during operation [1–3]. The semiconducting Bi₂Te₃-Bi₂Se₃ pseudo-binary alloys with a low content of Bi₂Se₃ have been known as one of the best n-type materials currently available for thermoelectric applications near room temperature. As the undoped Bi₂Te₃-Bi₂Se₃ single crystals are p-type semiconductors in the Bi₂Te₃-rich region [4–8], donor dopants such as SbI₃ and CuBr are usually doped to make n-type semiconductors.

Cooling capacity or the coefficient-of-performance of Peltier cooling modules is dependent on the figure-of-merit of the thermoelectric materials, which is determined by the thermoelectric properties such as Seebeck coefficient (α), electrical resistivity (ρ), and thermal conductivity (κ). As α , ρ , and κ are closely related to the electrical properties, it is necessary to characterize the variation of the thermoelectric properties with the dopant concentration to optimize the figure-of-merit of the thermoelectric materials [9, 10].

In this work, the Seebeck coefficient, electrical resistivity, and thermal conductivity of n-type 85% Bi₂Te₃-

15% Bi₂Se₃ single crystals doped with SbI₃ and CuBr were measured over the temperature range from 77 to 600 K. Also the effects of SbI₃ and CuBr doping on the reduced Fermi energy and the material factor of the 85% Bi₂Te₃-15% Bi₂Se₃ single crystals were characterized.

2. Experimental

High purity (99.999%) Bi, Te, and Se granules (~5 mm) were washed with 10% nitric acid, acetone, and distilled water to remove the surface oxide layer. The appropriate amounts of Bi, Te and Se were weighed to make 150 g of 85 mol % Bi₂Te₃-15 mol % Bi₂Se₃ and charged into a quartz tube with SbI₃ up to 0.20 wt % or CuBr up to 0.10 wt % as donor dopants. The inside wall of the quartz tube was carbon-coated by acetone cracking. The quartz tube was evacuated to 10^{-5} torr and sealed. Bi, Te and Se in the quartz tube were melted at 800 °C for 10 hours using a rocking furnace to ensure the composition homogeneity, and quenched to room temperature. The 85% Bi₂Te₃-15% Bi₂Se₃ ingots were then grown in a Bridgeman furnace at 850 °C with a growth rate of 1.2 mm/min and a temperature gradient of 25 °C/cm at the solid/liquid interface.

The grown ingots have the (1 1 1) cleavage planes aligned parallel to the growth direction, and two types of

specimens, $5 \times 5 \times 12$ (mm³) for thermoelectric measurement and $5 \times 5 \times 0.3$ (mm³) for Hall measurement, were cut along the growth direction. The electrical resistivity and Hall mobility of the SbI₃ and CuBr-doped 85% Bi₂Te₃-15% Bi₂Se₃ single crystals were characterized at temperatures ranging from 77 K to 600 K using Hall measurements with an AC magnetic field of 3000 gauss. The Seebeck coefficient was measured by the heat-pulse method [11] and the thermal conductivity was determined by the Harman method [12]. The figure-of-merit (Z) was determined using the relationship $Z = \alpha^2/(\rho \cdot x)$

3. Results and discussion

The Hall mobility ($\mu_H = R_H \cdot \sigma$) as a function of $(1/T)$ for the undoped, SbI₃-doped and CuBr-doped 85% Bi₂Te₃-15% Bi₂Se₃ single crystals is shown in Fig. 1. Compared to the undoped p-type specimen, the SbI₃ and CuBr-doped specimens have lower Hall mobility due to the impurity scattering [5]. At low temperatures, the Hall mobility of SbI₃ and CuBr-doped specimens decreased linearly along one line with increasing temperature regardless of the type and concentration of the dopant, and the Hall coefficient, not shown here, was constant up to 300 K, i.e. the electron concentration is saturated in this temperature range. For n-type semiconductors, it is reasonable to assume that the Hall mobility μ_H is equal to the electron mobility μ_e in the carrier saturation region [13]. From Fig. 1, the temperature dependence of the electron mobility of the SbI₃ and CuBr-doped specimens was obtained as

$$\log \mu_e = 0.90 \log(1000/T) + 1.771 \quad (1)$$

Although there was some deviation, the Hall mobility of the undoped specimen was also proportional to $T^{-0.9}$. Because the temperature dependence of the carrier mo-

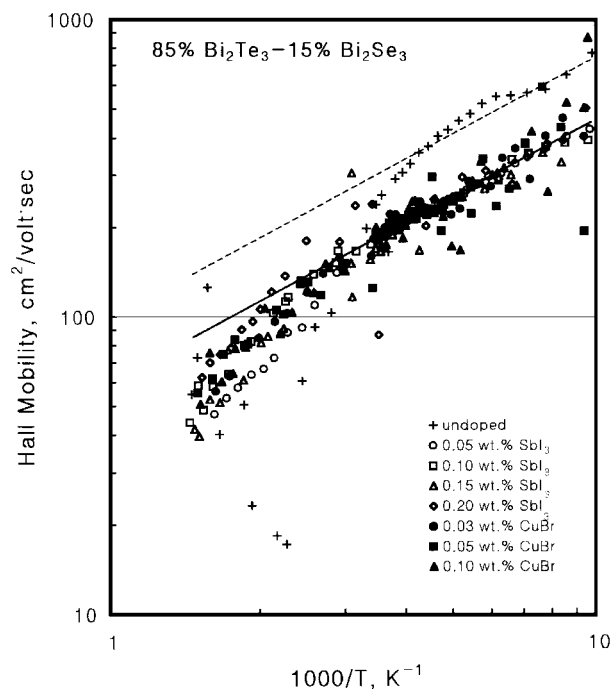


Figure 1 Hall mobility of the undoped, SbI₃-doped and CuBr doped 85% Bi₂Te₃-15% Bi₂Se₃ single crystals as a function of temperature.

bility can be expressed as a function of the scattering parameter s as $\mu \propto T^{(s-1)}$ [2], the scattering parameter of the 85% Bi₂Te₃-15% Bi₂Se₃ alloy was determined as 0.1.

Figs 2 and 3 illustrate the temperature dependence of the electrical resistivities ρ of the SbI₃ and CuBr-doped specimens, which could be understood with the Hall mobility data shown in Fig. 1. The increase of the electrical resistivity with increasing the temperature in the low temperature region was mainly attributed to the temperature dependence of the carrier mobility.

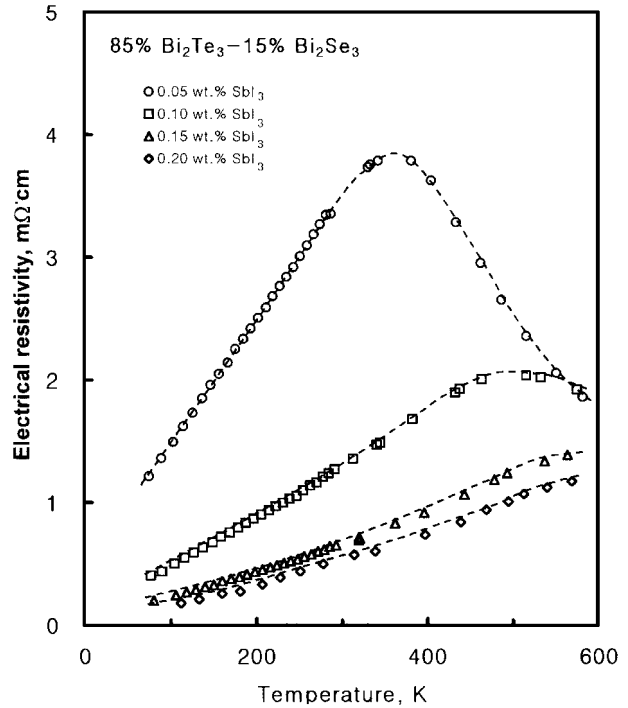


Figure 2 Electrical resistivity of the SbI₃-doped 85% Bi₂Te₃-15% Bi₂Se₃ single crystals as a function of temperature.

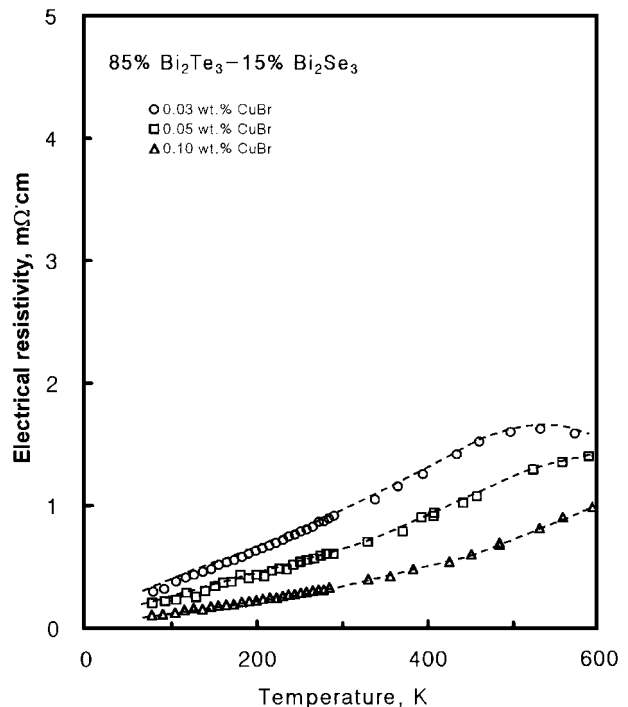


Figure 3 Electrical resistivity of the CuBr-doped 85% Bi₂Te₃-15% Bi₂Se₃ single crystals as a function of temperature.

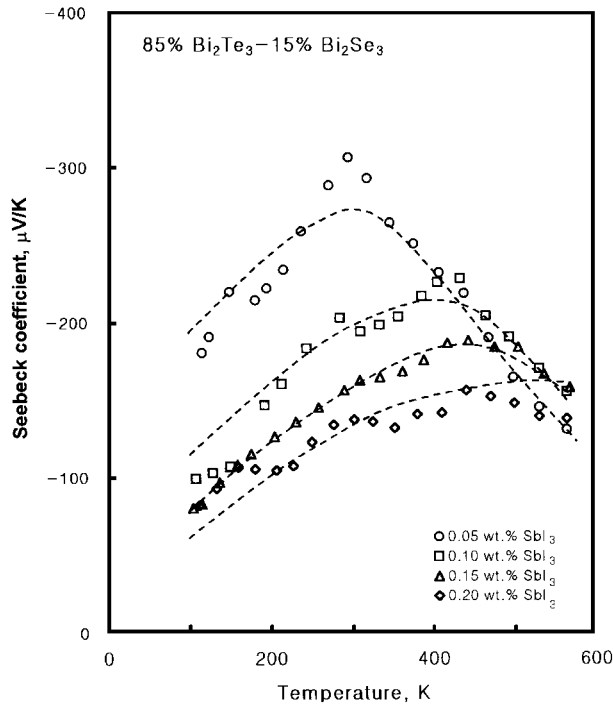


Figure 4 Seebeck coefficient of the SbI_3 -doped 85% Bi_2Te_3 -15% Bi_2Se_3 single crystals as a function of temperature.

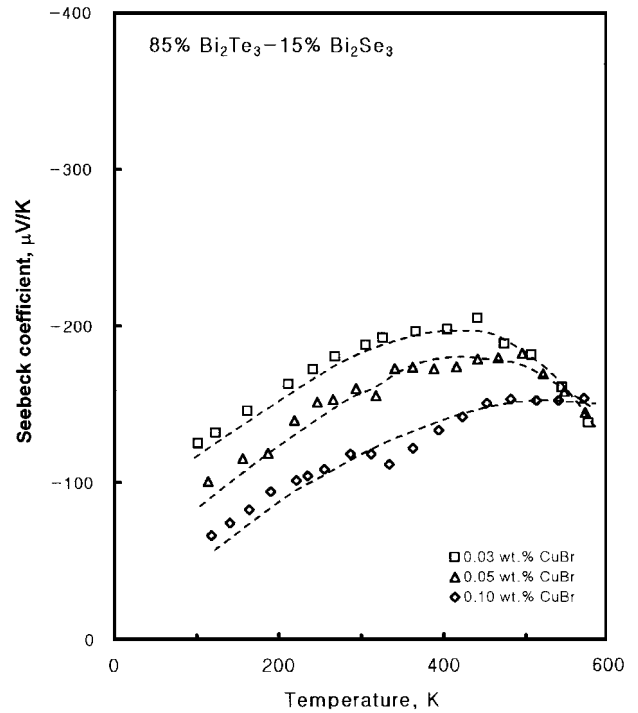


Figure 5 Seebeck coefficient of the CuBr -doped 85% Bi_2Te_3 -15% Bi_2Se_3 single crystals as a function of temperature.

With increasing temperature, the electrical resistivity of the lightly doped specimens decreased after reaching a maximum due to the occurrence of the mixed conduction [13]. The transition temperature from the extrinsic to the intrinsic conduction shifted to higher temperature with increasing dopant concentration. The specimens doped with SbI_3 more than 0.15 wt % or CuBr more than 0.05 wt % exhibited the extrinsic behavior at the temperature range investigated in this study.

Figs 4 and 5 illustrate the variations of the Seebeck coefficient α with temperature for the SbI_3 and CuBr -doped specimens, respectively. With increasing temperature, the Seebeck coefficient initially increased and then decreased after reaching a maximum value. With the increase of the amount of SbI_3 or CuBr doping, the maximum value of the Seebeck coefficient decreased and the temperature at which the Seebeck coefficient has its maximum shifted to higher temperature [14]. Such increase of the Seebeck coefficient at lower temperatures is due to the decrease of the electron mobility with temperature at the carrier saturation region. The decrease of the Seebeck coefficient at higher temperatures is associated to the occurrence of the mixed conduction. According to the Fermi-Dirac statistics, the Seebeck coefficient can be expressed as Equation (2) with the reduced Fermi energy ξ and the scattering parameter s . The Fermi integral $F_r(\xi)$ is expressed as Equation (3) [1, 9, 10].

$$\alpha = \pm \left(\frac{k_B}{e} \right) \left(\frac{(s + 5/2)F_{s+3/2}(\xi)}{(s + 3/2)F_{s+1/2}(\xi)} - \xi \right) \quad (2)$$

$$F_r(\xi) = \int_0^\infty \frac{x^r dx}{1 + \exp(x - \xi)} \quad (3)$$

In a thermoelectric material subjected to a temperature gradient, the Seebeck coefficient is related to the electrical potential gradient between the hot region and cold region. Thus, the temperature dependence of the Seebeck coefficient is dependent on the variation of the Fermi energy with temperature [10]. The scattering parameter of the SbI_3 and CuBr -doped specimens was determined as 0.1 in this study. Substituting $s = 0.1$ into Equations (2) and (3), the relationship between the Seebeck coefficient α and the reduced Fermi energy ξ was determined as Fig. 6. Then, the reduced Fermi energy of the SbI_3 and CuBr -doped specimens could be obtained from the measured Seebeck coefficient in Fig. 4, and was illustrated in Fig. 7 as a function of temperature. The reduced Fermi energy of the SbI_3 and CuBr -doped specimens became higher with increasing doping amount, which was due to the increase of the carrier concentration with increasing SbI_3 and CuBr doping. In general, the 85% Bi_2Te_3 -15% Bi_2Se_3 single

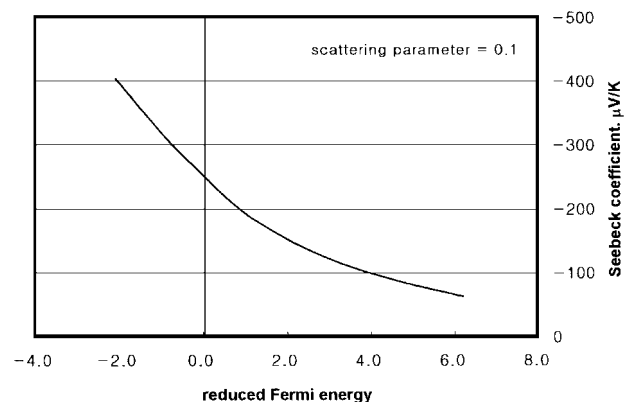


Figure 6 Relationship between Seebeck coefficient and reduced Fermi energy for $s = 0.1$.

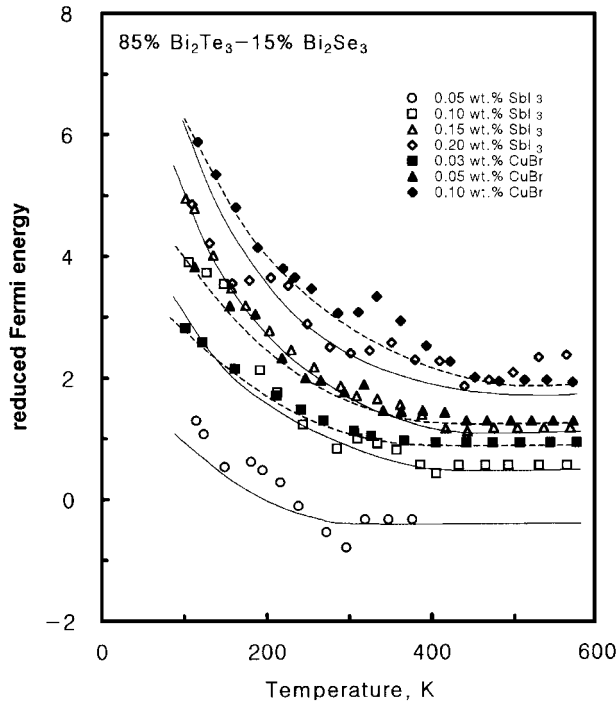


Figure 7 The reduced Fermi energy of the SbI₃ and CuBr-doped 85% Bi₂Te₃-15% Bi₂Se₃ single crystals as a function of temperature.

crystals exhibited heavy degeneracy in the low temperature region. However, the reduced Fermi energy was about 0~2 at temperatures above room temperature, indicating the SbI₃ and CuBr-doped specimens were partially degenerated semiconductors at these temperatures.

With the Fermi-Dirac statistics, the relationship between the carrier mobility and the electrical conductivity can be expressed as Equation (4) [9, 10].

$$\left(\frac{m^*}{m_0}\right)^{3/2} \cdot \mu_c = \frac{1605\sigma}{T^{3/2}F_{(s+1/2)}(\xi)} \quad (4)$$

In Equation (4), m^* and m_0 is the effective mass and rest mass of the electron, respectively. Fig. 8 illustrate $\log(m^*/m_0)^{3/2} \mu_c$ of the undoped, SbI₃-doped and CuBr-doped specimens as a function of $\log T$. For the undoped, SbI₃-doped and CuBr-doped specimens, $\log(m^*/m_0)^{3/2} \mu_c$ decreased with increasing $\log T$ linearly along the lines with the same slope, and the temperature dependence of $(m^*/m_0)^{3/2} \mu_c$ in 85% Bi₂Te₃-15% Bi₂Se₃ could be expressed as $(m^*/m_0)^{3/2} \mu_c \propto T^{-1.7}$. As shown in Fig. 8, $(m^*/m_0)^{3/2} \mu_c$ of 85% Bi₂Te₃-15% Bi₂Se₃ increased with doping of SbI₃ and CuBr. The material factor (β) of a thermoelectric material is expressed as Equation (5) [15].

$$\beta = \left(\frac{m^*}{m_0}\right)^{3/2} \cdot \frac{\mu_c}{(x - x_{el})} \quad (5)$$

The lattice thermal conductivity ($k - k_{el}$) of 85% Bi₂Te₃-15% Bi₂Se₃ would not be varied with doping of SbI₃ and CuBr. Compared to the SbI₃-doped specimens, the CuBr-doped specimens exhibited higher $(m^*/m_0)^{3/2} \mu_c$, which implied that CuBr doping is more

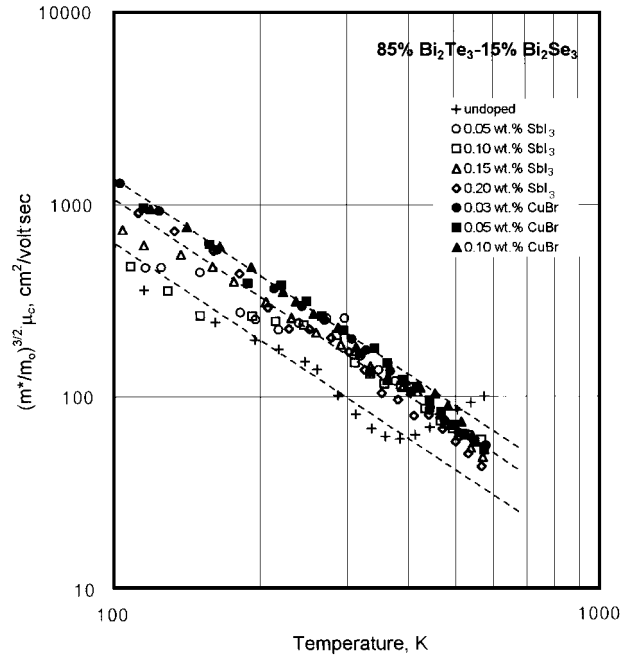


Figure 8 $\log(m^*/m_0)^{3/2} \mu_c$ of the undoped, SbI₃-doped and CuBr-doped 85% Bi₂Te₃-15% Bi₂Se₃ single crystals as a function of $\log T$.

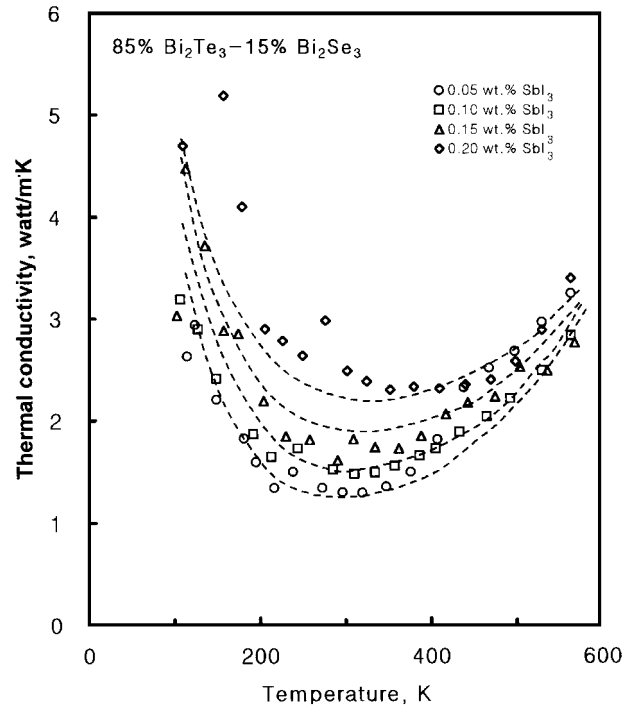


Figure 9 Thermal conductivity of the SbI₃-doped 85% Bi₂Te₃-15% Bi₂Se₃ single crystals as a function of temperature.

effective to improve the material factor and thus the figure-of-merit of 85% Bi₂Te₃-15% Bi₂Se₃. As shown in Fig. 1, the Hall mobility of 85% Bi₂Te₃-15% Bi₂Se₃ was proportional to $T^{-0.9}$. From this, the temperature dependence of the effective mass in 85% Bi₂Te₃-15% Bi₂Se₃ was found to be $(m^*/m_0)^{3/2} \propto T^{-0.8}$.

Figs 9 and 10 illustrate the thermal conductivity of the SbI₃ and CuBr-doped specimens as a function of temperature, respectively. With increasing temperature, the thermal conductivity initially decreased and then increased after reaching its minimum value. At the same temperature, the thermal conductivity increased with

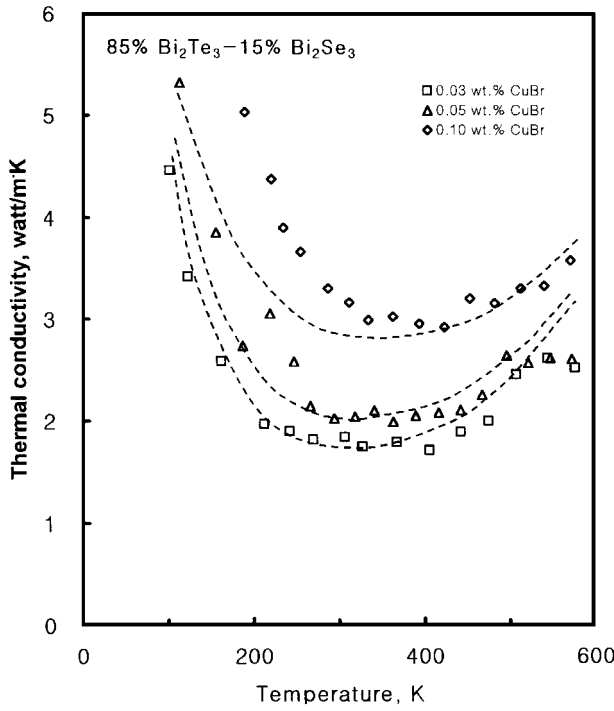


Figure 10 Thermal conductivity of the CuBr-doped 85% Bi₂Te₃-15% Bi₂Se₃ single crystals as a function of temperature.

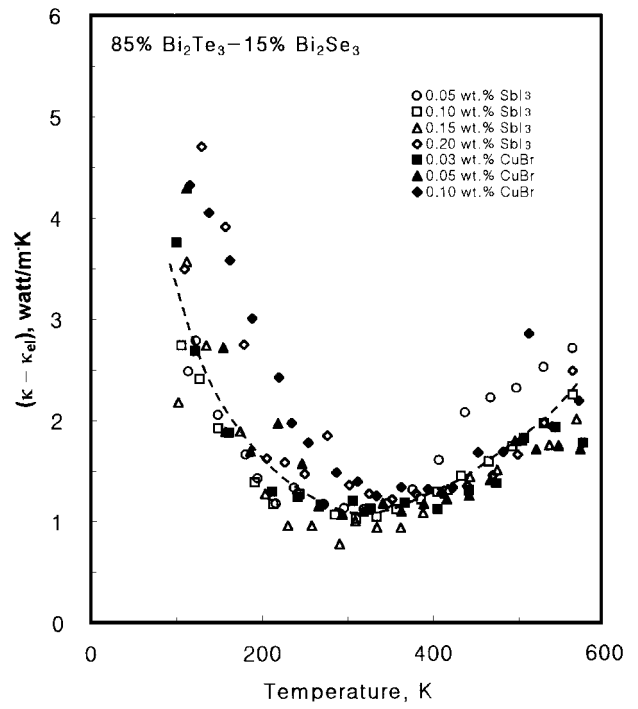


Figure 11 $(k - k_{el})$ of the SbI₃ and CuBr-doped 85% Bi₂Te₃-15% Bi₂Se₃ single crystals as a function of temperature.

increasing SbI₃ or CuBr doping. With Widemann-Franz law, the electrical contribution to the thermal conductivity is expressed as $k_{el} = LaT$ where L is the Lorentz number and can be determined with Equation (6) [9, 16].

$$L = \left[\frac{(s + 7/2)F_{s+5/2}(\xi)}{(s + 3/2)F_{s+1/2}(\xi)} - \left[\frac{(s + 5/2)F_{s+3/2}(\xi)}{(s + 3/2)F_{s+1/2}(\xi)} \right]^2 \right] \left(\frac{k_B}{e} \right)^2 \quad (6)$$

$(k - k_{el})$ values of the SbI₃ and CuBr-doped specimens were determined with the Lorentz number L which was calculated by substituting the reduced Fermi energy (Fig. 6) and also the scattering parameter $s = 0.1$ into Equation (6). As shown in Fig. 11, $(k - k_{el})$ values of the SbI₃ and CuBr-doped specimens fit into one curve regardless of the dopant concentration. With increasing temperature, $(k - k_{el})$ decreased at low temperature region and then increased at temperatures above 300 K [17].

The figure-of-merits $Z (= a^2/\sigma k)$ of the SbI₃ and CuBr-doped specimens are illustrated in Fig. 12 and Fig. 13, respectively. The figure-of-merit increased initially with increasing temperature, showed a maximum at 250 ~ 300 K, and then decreased with further increase in the temperature. Low figure-of-merit at low temperature region was owing to high lattice thermal conductivity, and low Seebeck coefficient at high temperature region caused the figure-of-merit to decrease [18]. Although the electrical resistivity decreased with increasing SbI₃ and CuBr doping, the Seebeck coefficient decreased simultaneously, implying that an optimum amount of SbI₃ and CuBr doping exists to im-

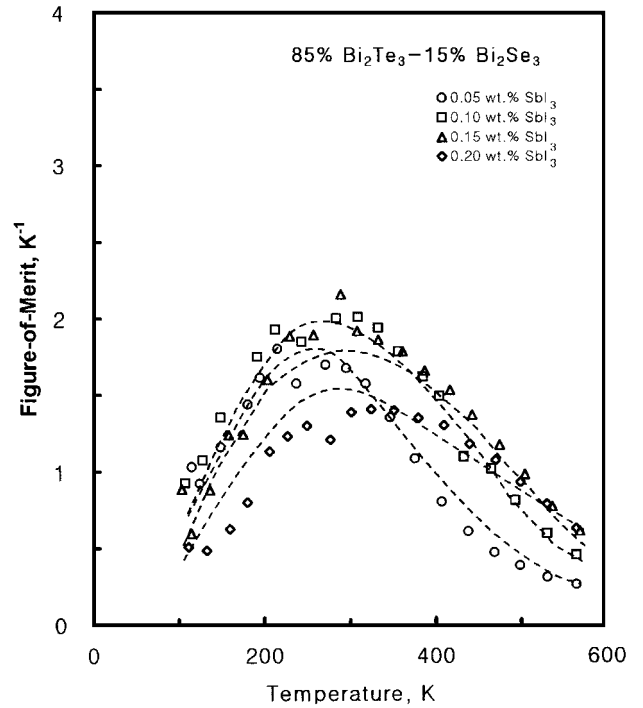


Figure 12 Figure-of-merit of the SbI₃-doped 85% Bi₂Te₃-15% Bi₂Se₃ single crystals as a function of temperature.

prove the figure-of-merit of 85% Bi₂Te₃-15% Bi₂Se₃. With increasing SbI₃ and CuBr doping, the temperature at which the figure-of-merit has a maximum shifted to higher temperature due to the increase of the electron concentration [19]. A maximum figure-of-merit of $2.0 \times 10^{-3}/K$ and $2.2 \times 10^{-3}/K$ was obtained for 0.1 wt % SbI₃-doped specimen and 0.03 wt % CuBr-doped specimen, respectively.

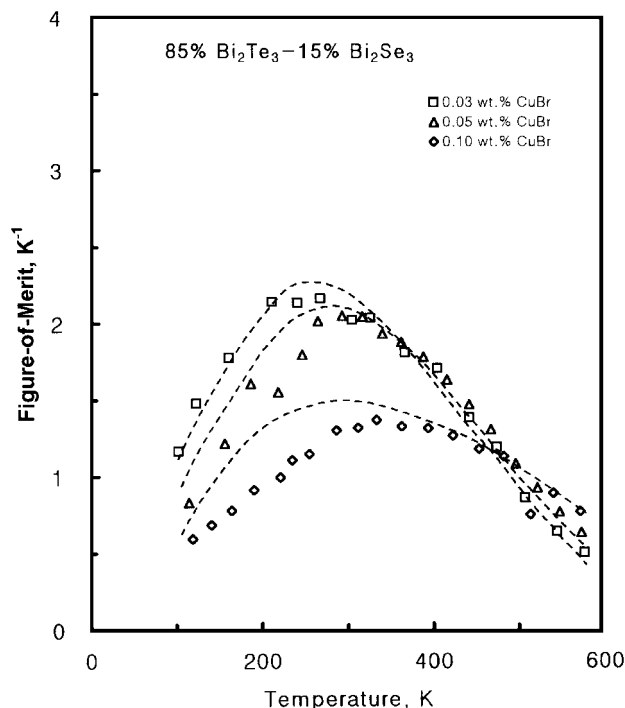


Figure 13 Figure-of-merit of the CuBr-doped 85% Bi₂Te₃-15% Bi₂Se₃ single crystals as a function of temperature.

4. Conclusions

By characterizing the Hall mobility, Seebeck coefficient, electrical resistivity, thermal conductivity and figure-of-merit of 85% Bi₂Te₃-15% Bi₂Se₃ single crystal with the amount of SbI₃ and CuBr doping, the following conclusions can be made in this study:

1. The scattering parameter in 85% Bi₂Te₃-15% Bi₂Se₃ single crystal was determined to be 0.1 from the temperature dependence of the carrier mobility.
2. With increasing SbI₃ or CuBr addition, the Seebeck coefficient decreased and the temperature of the maximum Seebeck coefficient, which is the onset of the mixed conduction, shifted to higher temperature.
3. Compared to the SbI₃-doped specimens, the CuBr-doped specimens exhibited higher $(m^*/m_0)^{3/2}\mu_c$, implying that CuBr is a more effective dopant to improve the material factor and thus the figure-of-merit.
4. With increasing SbI₃ and CuBr doping, the temperature at which the figure-of-merit has a maximum

shifted to higher temperature due to the increase in the electron concentration.

5. The maximum figure-of-merit of $2.0 \times 10^{-3}/K$ and $2.2 \times 10^{-3}/K$ was obtained for 0.1 wt % SbI₃-doped specimen and 0.03 wt % CuBr-doped specimen, respectively.

References

1. D. M. ROWE, in "CRC Handbook of Thermoelectrics" (CRC Press, Inc., Boca Raton, 1995) p. 617.
2. A. F. IOFFE, in "Semiconductor Thermoelements and Thermoelectric Cooling" (Infosearch, London, 1957) p. 155.
3. J. W. VANDERSANDE and J.-P. FLEURIAL, in Proceedings of the 15th International Conference on Thermoelectrics, Pasadena, California, March 1996, edited by Thierry Caillat (1996) p. 252.
4. R. G. COPE and A. W. PENN, *J. Mater. Sci.* **3** (1968) 103.
5. D. B. HYUN, H. P. HA and J. D. SHIM, in Proceedings of the 11th International Conference on Thermoelectrics, Arlington, Texas, October 1992, edited by K. R. Rao (1992) p. 266.
6. D. L. GREENAWAY and G. HARBEKE, *J. Phys. Chem. Solids* **26** (1965) 1585.
7. J. BLACK, E. M. CONWELL, L. SEIGEL and C. W. SPENCER, *J. Phys. Chem. Solids* **2** (1957) 240.
8. H. KAIBE, M. SAKATA, Y. ISODA and I. NISHIDA, *J. Jpn. Inst. Metals* **53** (1989) 958.
9. H. J. GOLDSMID, in "Thermoelectric Refrigeration" (Plenum Press, New York, 1964) p. 134.
10. D. M. ROWE and C. M. BHANDARI, in "Modern Thermoelectrics" (Holt, Rinehart and Winston, London, 1983) p. 7.
11. P. C. EKLUND and A. K. MABATAH, *Rev. Sci. Instrum.* **48** (1977) 775.
12. T. C. HARMAN, J. H. CAHN and M. J. LOGAN, *J. Appl. Phys.* **30** (1959) 1351.
13. K. SEEGER, in "Semiconductor Physics" (Springer-Verlag, New York, 1982) p. 46.
14. L. C. BENNETT and J. R. WIESE, *J. Appl. Phys.* **32** (1961) 562.
15. C. H. CHAMPNESS, W. B. MUIR and P. T. CHIANG, *Can. J. Phys.* **45** (1967) 3611.
16. R. IONESCU, J. JAKLOVSZKY, N. NISTRO and A. CHICULITA, *Phys. Stat. Sol. (a)* **27** (1975) 27.
17. H. KAIBE, Y. TANAKA, M. SAKATA and I. NISHIDA, *J. Phys. Chem. Solids* **50** (1989) 945.
18. C. B. SATTERTHWAITE and R. W. URE, JR., *Phys. Rev.* **108** (1957) 1164.
19. W. M. YIM, E. V. FIZKE and F. D. ROSI, *J. Mater. Sci.* **1** (1966) 274.

Received 5 December 1997
and accepted 16 July 1998